Available online at www.sciencedirect.com

ScienceDirect

Procedia Materials Science 9 (2015) 450 – 459

Procedia Materials Science

www.elsevier.com/locate/procedia

International Congress of Science and Technology of Metallurgy and Materials, SAM – CONAMET 2014

Micro and nanostructured phases obtained by mechanical alloying - low temperature annealing in AB_5-H_2 systems

Sergio A. Obregón[a,b,c], Eugenia Zelaya[a,d], Marcelo R. Esquivel[a,b,d,*]

[a] *Consejo Nacional de Investigaciones Científicas y Técnicas, Avda. Bustillo km 9.5, Bariloche, (8400), Argentina*
[b] *Centro Regional Universitario Bariloche, UNComa, Quintral 1250, Bariloche (8400), Argentina*
[c] *Instituto Balseiro, UNCuyo, Avda Bustillo km 9,5 (8400), Argentina.*
[d] *Centro Atómico Bariloche, Comisión Nacional de Energía Atómica, Avda. Bustillo km 9.5 Bariloche (8400), Argentina*

Abstract

In this work, the characteristics of a commercial sample of $LaNi_5$ are compared to those of an experimental one obtained by mechanical alloying followed by low temperature annealing. The nominal composition of the experimental sample is Mm-4Ni-1Al where Mm =$La_{0.25}Ce_{0.52}Nd_{0.17}Pr_{0.06}$. The morphology, nano, micro and structure of each sample are analyzed. Morphology is analyzed by both SEM and TEM. Micro and structure were studied by XRD and nanostructure by TEM. To the detection limits, the commercial sample is a mono phase. The mono phase possesses good crystalline characteristics closely related to samples obtained at annealing in near equilibrium conditions (T > 800 °C, t > 48 h). The Mm-4Ni-1Al sample has an AB_5 structure as a major phase. The minor phases were characterized by XRD and TEM. The analysis is completed with the study of the hydrogen sorption properties of each sample. Finally, both types of properties are correlated. The opportunities of improvement of the synthesis method are discussed in relation to the investment costs of each production technique.

Peer-review under responsibility of the Scientific Committee of SAM–CONAMET 2014

Keywords: TEM, SEM, XRD, Thermal compression of hydrogen

* Corresponding author. Tel.: +54-02944-445139; fax: +54-02944-445290.
E-mail address: esquivel@cab.cnea.gov.ar

Peer-review under responsibility of the Scientific Committee of SAM–CONAMET 2014
doi:10.1016/j.mspro.2015.05.016

1. Introduction

Nomenclature

D	crystallite size, Å
IM	intermetallic compound
R	Ball mass to sample mass ratio, dimensionless
t	time, h
t_{im}	integrated milling time, h
T	temperature, °C
TCH	thermal compression of hydrogen
s	deformation of the cell parameter, %.

The replacement of each unitary operation related to fossil fuel technology for each equivalent of the hydrogen technology demands a specific quantity and type of requirements. The requirements include the development of a reachable scenario for both the technology and economic possibilities of the host country. This really means that the replacement is effective only if the afore mentioned conditions are mature enough to be fulfilled. In the current case of the gasoline service stations of fossil fuels economy, the thermal hydrogen compressors are the natural replacement associated to the hydrogen technology. In developing countries as Argentina, this technological replacement should consider the economics, cultural and social advances and technological limitations of the country. The last one refers both to conditions of synthesis of the desired intermetallic compound (IM) and to the performance and stability under operation of the thermal compressor of hydrogen.

Unlike traditional gas compressors with moving parts, this device is based on the reversibility of the hydride formation and the function ability of this reaction with both pressure and temperature as published by Huston and Sandrock (1980), Lotoskyy et al. (2014) and Obregón and Esquivel (2014). Then, the operation is limited to the absorption/desorption of hydrogen to/from a solid structure inside an insulated container as presented by Obregon and Esquivel (2014). Therefore, due to their intrinsic operation characteristics, the synthesis and production of the IM are the limiting conditions for the insertion of TCH in the alternative (hydrogen-based one) energetic matrix of the country.

The design of the IM synthesis process must involve the microstructure, structure and morphological properties to correlate them with the proper performance of the compressor. A simple way to optimize the production costs of the IM is to define an appropriate frame of both technological and economical limitations. Once those factors are selected, the synthesis process might be well defined.

In this work, materials for TCH are obtained by mechanical alloying followed by low temperature annealing ($T < 600$ °C). The mentioned combined process was defined in a previous work by Obregón et al. (2012). The process defines a working frame where the appropriate microstructure of the AB_5 can be obtained within constrained values for both T and t as published by Obregón et al. (2012).

The morphology, microstructure and structure of experimental samples are compared to those of commercial ones to compare properties and to analyze the possibilities of use in TCH. The main aim of the work is to enhance the synthesis, annealing process and use of the IM in the desired technological application.

2. Materials and experimental.

Experimental sample was obtained by low energy mechanical alloying in a Uni-Ball Mill II (Australian Instruments). Sample was synthesized from a nominal mixture of $La_{0.25}Ce_{0.52}Nd_{0.17}Pr_{0.06}$-4Ni-1Al. Reactants were Mischmetal (lantanides alloy, Alfa AEesar, 99.6%), Ni (Sigma Aldrich, 99.99%) and Al (Aldrich, 99.99%). Ball mass to sample mass ratio selected is R = 12. Integrated milling time (t_{im}) was 148 h. Commercial sample selected for comparison was $LaNi_5$ (Reacton, 99.6%). Microstructure and structure of samples was analyzed by XRD using PW1701 and PANanalytical Empyrean diffractometers. Microstructure was analyzed assuming that the diffraction peaks were a convolution of the Gauss and Lorentz functions as described by Langford et al. (1998).

Crystallographic structures were refined by the Rietveld method using Fullprof program as cited by Rodriguez-Carvajal, (1990). Particle size distribution and morphology were studied by scanning electron microscopy (SEM) using a Philips 515 SEM microscope. Nanostructure was analyzed by transmission electron microscopy (TEM) using a FEI CM 200UT operated at 200 keV. Elemental composition was verified by energy dispersive spectroscopy (EDS) with devices associated to SEM/TEM microscopes. Hydrogen sorption properties were studied in a Sievert type device designed ad-hoc.

3. Results and discussion

3.1. Nano, micro and structure of samples

SEM images of the samples are presented in Fig. 1. Commercial sample is shown in Fig. 1.a and experimental one in Fig. 1.b. The differences in morphology are clearly observed. Commercial sample presents smooth surfaces with sharp edges. This morphology is associated to high temperature (T > 800 °C) and long (t > 48 h) synthesis methods. In these methods, both temperature and time are large enough to allow the diffusion of atoms from the bulk of the solid to surface to allow a good homogeneous composition. This behavior is well evaluated by observing the smooth surfaces. Sharp edges correspond to cuts done to the fragile IM of the sample in order to be observed in the SEM microscope.

Sample obtained by low energy mechanical alloying followed by low temperature annealing is clearly different. The surface is not smooth and the quality of the surface is less developed than that of the commercial sample. Fracture and cold welding left the surface with uneven layers and borders as reported by Cerón-Hurtado and Esquivel (2010) and Lu and Lai (1998). Traces of cold welding, promoted by successive folding of layers of the sample are indicated by hollow arrows and traces of fracture due to impacts on the fragile structure by full arrows.

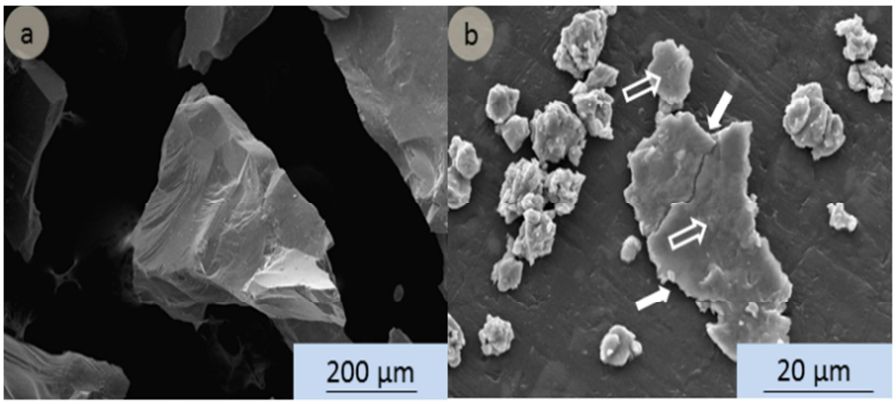

Fig.1. SEM images (a) Commercial sample; (b) Experimental sample.

The diffractograms of each sample are presented in Fig. 2. Commercial and experimental correspond to Figs. 2.a. and 2.b, respectively. The first one presents only the AB_5 phase to the detection limits of the technique. All peaks in pattern were indexed according to $LaNi_5$ structure. This structure is the most representative of this family of IM´s. The sample presents a well-developed crystalline structure. Peaks are thin with a large maximum height/background ratio. The crystalline features can be characterized by microstructural parameters *D* and *s*. *D* and *s* stand for crystallite size and cell parameter deformation, respectively. A summary of values are shown for a selected hkl directions in Table 1. As observed, these values are in agreement with the profile of Fig.. 1.a. *D* values are larger than 400 Å and *s* values smaller than 2 %. The phase presents preferential orientation in the 101 directions. This assessment is deduced by comparing the relative intensities of this family of directions with those of the theoretical $LaNi_5$ structure (not shown here).

The diffractogram of the experimental sample is different from that of the commercial sample. In addition to the displacement of the main peaks of the AB_5 structure, the peaks show a peak/background ratio smaller than that of

$LaNi_5$ of Fig. 1(a). Sample is not single phase. All phases identified are shown in Fig. 1(b). The main phase is $MmNi_{4.25}Al_{0.75}$. The elemental composition of the compound was calculated using a crystallographic-sustitutional model developed ad-hoc for this structure by Obregón et al (2012). Besides the main phase, the following ones were also detected: Ni_3Al, Mm y Mm_7Ni_3. The structure characteristics are summarized in Table 2.

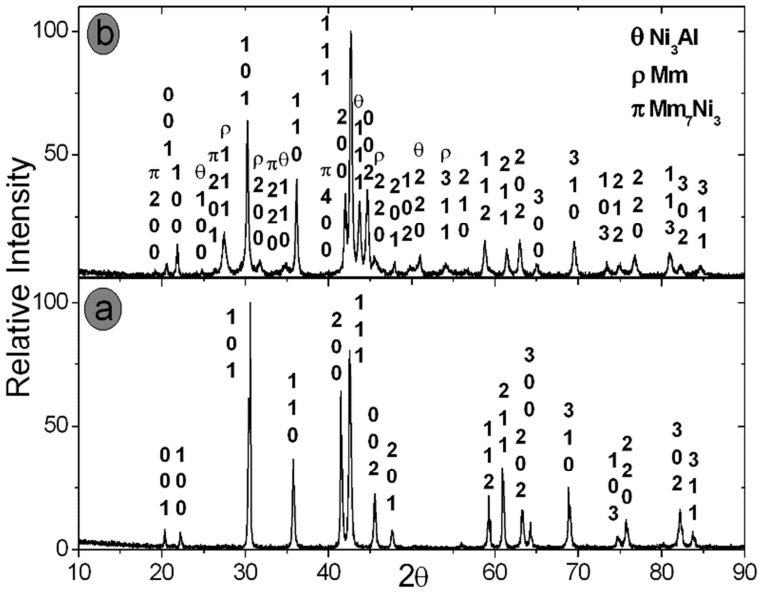

Fig. 2 (a). Diffractogram of commercial sample; (b). Diffractogram of experimental sample.

For $MmNi_{4.25}Al_{0.75}$, the *D* and *s* parameters were calculated for the same hkl directions than those calculated for $LaNi_5$. The values are shown in Table 1. The straightforward comparison between both groups of values indicates that crystalline features are better for $LaNi_5$ than for $MmNi_{4.25}Al_{0.75}$. From the profile of Fig. 2(b), it is also deduced that the phases summarized in Table 2 present microstructural parameters similar to $MmNi_{4.25}Al_{0.75}$.

Table 1. Microstructural values of AB_5 phases.

Phase	hkl	*D* (Å) ± 10	*s* (%)
	100	640	0.03
$LaNi_5$	001	430	0.05
	110	480	0.03
	100	400	0.15
$MmNi_{4.25}Al_{0.75}$	001	400	0.15
	110	400	0.15

A further look in the experimental sample of Fig. 2(b) indicates that the background is relatively high with wide peaks under the main ones with Δθ ranges larger than 3°. This particular shape of the profile suggests that the sample has nanostructured phases.

Table 2. Characteristics of the phases present in the sample.

Phase	Space Group	Structural parameters	
		a, b, c ± 0.005	α,β,γ
$MmNi_{4.25}Al_{0.75}$	*P6/mmm*	4.961, 4.050	90,90,120

Mm_7Ni_3	*P6₃mc*	10.191, 6.386	90,90,120
Mm	*Fm3m*	5.612	90,90,90
Ni_3Al	*Fm3m*	3.581	90,90,90

An example of these structures is shown in Fig. 3. TEM bright field and dark field images are shown in Figs. 3(a) and 3(b), respectively. Bright field image indicates that particles are agglomerated in sizes larger than 200 nm. The particles have rounded edges. These are produced due to the combined cycle of mechanical alloying. Surfaces are clearly faceted as a product of the annealing under Ar.

The dark field image shows crystalline domains smaller than 50 nm. Figure 4 shows the elemental composition of a particle similar to that of Fig. 3. This figure displays a spectrum corresponding to the EDS nano-analysis of the sample. It can be detected the presence of lanthanides, Ni and Al. The Cu peaks correspond to the TEM sample holder and the grid.

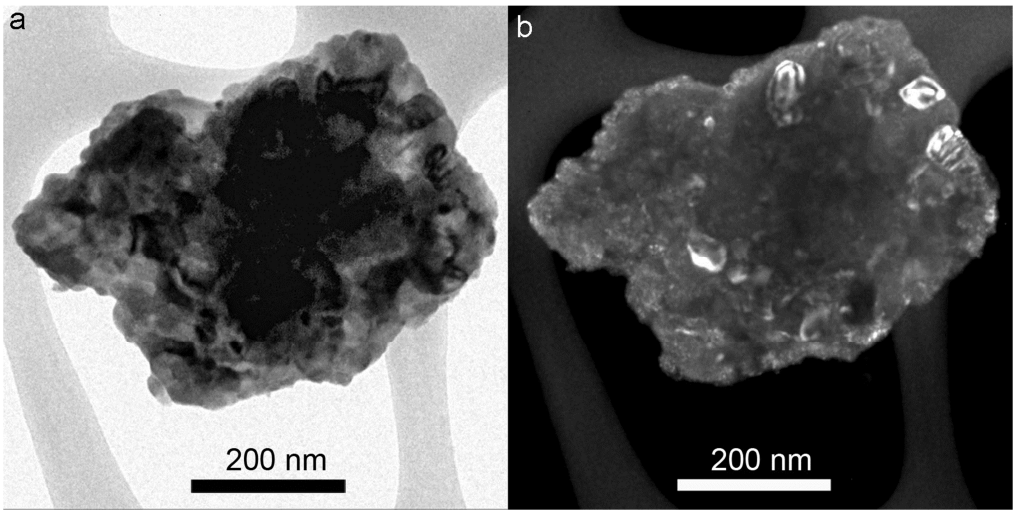

Fig. 3 (a). Bright field image. (b). Dark field image.

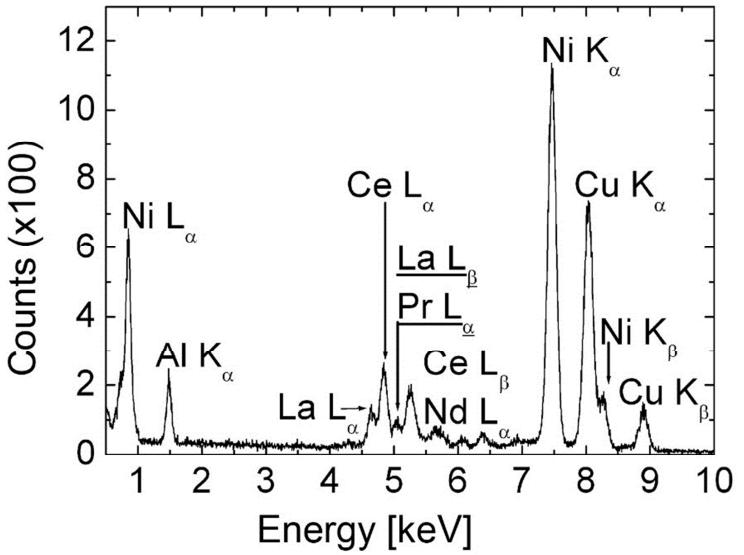

Fig. 4. EDS spectrum performed over a characteristic particle.

A selective area diffraction SAD pattern is shown in Fig. 5. The measurement was done to a particle with an EDS spectrum different to that of Fig. 3. Rings were indexed according to two structures: Ni and Mm. Ni was not detected by XRD. The SAD pattern shows that both structures have preferential orientation because rings of both structures have brighter dots than the rest of the characteristic ring.

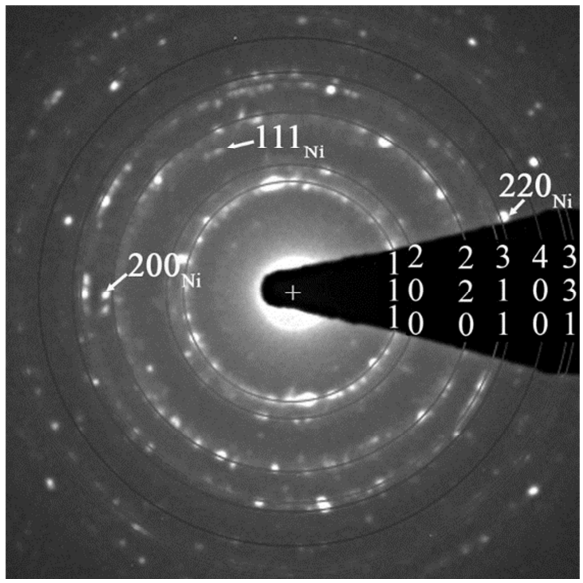

Fig. 5. SAD pattern. Mm (*Fm*3*m*) is indicated with light gray lines. Ni (*Fm*3*m*) with white full arrows.

Microstructural parameters of Mm (*Fm*3*m*) were calculated from 111 diffraction peak of Fig. 2 (b). Values obtained were $D = 170 \pm 10$ Å and $s = 0.6\%$.

The analysis of the results of Figs. 1-4 indicates that thermal annealing to high temperatures leads to a single phase sample with well-developed crystalline structure. In this case, this treatment led to a preferentially oriented sample. The references on the formation of nano-crystalline phases on IM obtained using these synthesis methods showed that the composition and structure are similar to the main phase as presented by Esquivel and Zelaya (2013).

Samples obtained by low energy mechanical alloying (LEMA) followed by low temperature annealing led to the formation of a composite containing the main AB_5 phase and the minor ones. To understand the formation of the composite the following facts should be considered:

1) LEMA occurs at T < 150 °C as discussed by Cerón-Hurtado and Esquivel (2010).
2) Melting temperatures (m.t) are 600 °C, 1400 °C and 795-1100°C for Al, Ni and Mm alloy, respectively. Mm m.t was reported by Palmer et al. (1992).
3) Diffusion processes are favored at temperatures higher than Tamman as presented by Merkle and Maier (2005).

Under these limiting conditions, diffusion processes in the solid bulk are not favored. This fact suggests that cold welding is produced locally forming secondary phases different from the AB_5. These phases have different mechanical and microstructural properties from the parent mixture of metals/alloys. Once obtained, these structures resist the milling stages without alloying to the main AB_5 phase. As a result, a composite is formed with a global composition similar to the starting nominal one. The composite is similar to the sample observed in Fig. 2 (b). Some of the phases have a well-developed crystalline structure as shown in Table 2 and Fig. 2. Other phases have less-developed crystalline features such as Ni shown in Fig. 5.

Mass sample percentage was calculated by the Rietveld method using Fullprof software. The results are summarized in Table 3. As deduced from the values, main phase is AB_5.

Table 3. Mass sample composition.

Phase	Mass percentage % ± 2
$MmNi_{4.25}Al_{0.75}$	63
Mm_7Ni_3	36
Mm, Ni_3Al, Ni	> 1

3.2 Hydrogen sorption properties

The PCT (pressure composition temperature) isotherms at room temperature are shown in Fig. 6. Figure shows hydrogen sorption properties for both samples. PCT main features are summarized in Table 4. It is clearly observed that commercial sample has a flatter plateau than experimental sample. This behavior is quantified by comparing the slope of the PCT´s as shown in fourth column of Table 4. Slope values are lower for commercial sample. The higher value for experimental sample is related to no completely relaxed surfaces with residual stress conditions. The presence of the other minor phases in the IM mixture also affects the hydrogen sorption properties. Ni might favor the kinetics by adding catalytic properties. The other phases (Ni_3Al, Mm_7Ni_3) might dissipate the heat of reaction. The hysteresis values are lower for $LaNi_5$ as shown in third column of Table 4. It means that absorption/desorption at these temperatures have less energetic losses. The max %M m/m is larger in the commercial sample. It indicates a maximum use of the mass sample. This feature is not decisive in static applications such as TCH.

The analysis of microstructure and sorption properties point out that the commercial sample have a more relaxed structure that allows near equilibrium hydrogen sorption interaction leading to better PCT curves as shown in Fig. 6 and Table 4.

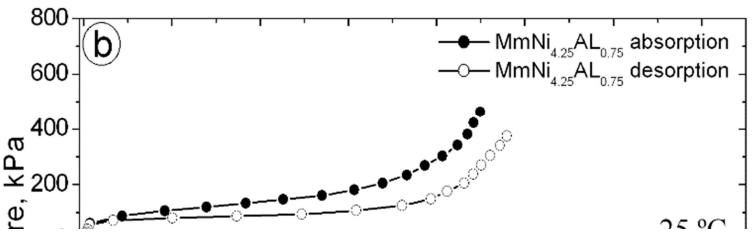

Fig. 6 Pressure composition isotherms

Table 4. Hydrogen sorption properties of AB_5 phases.

Phase	Peq ± 5 (kPa)	ln (P_a/P_d)	d (P)/%Hm/m	Max (%H m/m)
$MmNi_{4.25}Al_{0.75}$	120 (abs)	0.34	270	0.85 (abs)
	80 (des)		130	0.80 (des)
$LaNi_5$	270 (abs)	0.16	40	1.35 (abs)
	230 (des)		30	1.35 (des)

3.3 Alternative methods for synthesis and improvement of IM´s and application to TCH in Argentina.

IM´s for use in TCH in Argentina can be synthesized by two alternative methods:

1) High temperature methods at T > 800 °C for 24 to 48 h.
2) Mechanical alloying followed by low temperature annealing methods at T < 600 °C for 24 h.

The production of AB_5-based compounds using mechanical alloying-low temperature annealing treatment presents minor phases as co-products as obtained in this work and Obregón et al. (2012). These phases and the main AB_5 constitute a composite. Therefore, the individual compounds cannot be separated easily after synthesis. These minor phases affect the hydrogen sorption properties of the main AB_5 depending on the identity of the compound formed.

The use of reactants as fine powder previous to milling is an alternative to avoid the formation of these phases. It occurs because *initial stage* of milling is shortened suppressing fracture as dominant mechanism. It also leads to a short t_{im} values which reduces the costs of milling. This strategy implies buying largely expensive reactants. Alternatively, reactants can be milled previous to be processed/mixed in the mill. But that operation is not possible for lanthanide alloys in stainless steel/Agatha milling devices because of the selective lamination of these alloys on the milling media.

A third alternative involving the import of the IM to Argentina is no reasonable since these compounds and the dollar/peso ratio increased steadily in the last ten years. Among other conditions, this current situation occurs

because these $LaNi_5$-based compounds and their constituting elements became an important asset for producing countries as explained by Haves-Labruto et al. (2013). Since Argentina is not a producer of these commodities, the valid option is to import cheaper consumables (lanthanides and Ni in large pieces) and fabricate the AB_5. For this country, option 2 represents a reachable production method with low energy consumption.

Nevertheless, it must be kept in mind that the AB_5 is destined to TCH. This application is not focused on movile devices but static ones with no strict limitations in (%mH/m device). Therefore, the formation of minor phases is not a limitation for the sample. In fact, free-Ni can catalyze the hydrogen absorption/desorption process. But the presence of these phases and the microstructure of the main AB_5 should be controlled in order to obtain PCT with no extremely large slopes that might compromise the compression cycle as explained by Cerón-Hurtado and Esquivel (2012) and Obregón and Esquivel (2014).

4. Summary and conclusions

In a previous work, the production costs were compared for IM´s using both alternative 1 and 2 at laboratory scale. Work was reported by Obregón et al. (2012). In that research, it was concluded that the costs of production of the second option were comparatively lower than those of the first option. This conclusion means that it is valid to pursue an investigation path focused on the decrement of costs necessary to achieve the replacement of the fossil fuel technology by their equivalents of the hydrogen technology. This strategy implies the search of lower technological requirements and cheaper economical resources. The investment costs are necessarily lower for technologies with treatments at $T < 600$ °C than those at $T > 800$ °C.

As obtained in this work, the synthesis of IM by mechanical alloying-low energy milling leads to the formation of a main AB_5 phase and minor ones. Since the AB_5 is destined to TCH, the presence of these minor phases is not necessarily a drawback. In fact, free nanostructured Ni helps the sorption processes. Nevertheless, it should be kept in mind that the IM is ultimately destined to TCH. Therefore, the quality of the IM including minor phases and microstructure of the main IM should be good enough to assure the compression cycle of the TCH device as discussed by Esquivel (2013).

Acknowledgements

Sergio Obregón thanks CONICET for the Doctoral Grant. The authors wish to thank ANPCyT (PICT 0092), CONICET (PIP 0109) and UNComa (O4/B183) for partial financial support.

References

Ceron-Hurtado, N.M., Esquivel, M.R., 2010. Stages of mechanical alloying during the synthesis of Sn-containing AB_5-based intermetallics. International Journal of Hydrogen Energy 35, 6057-6062.

Esquivel, M.R., 2013. Characterization of materials obtained by an innovative integrated synthesis method aimed to the hydrogen technology. In "X-Ray Diffraction: Structure, Principles and Applications. In Shih, K. (Ed). Nova Publishers, New York, 183-206.

Esquivel, M.R., Zelaya, E., 2013. Aplicación práctica de intermetálicos a compresión térmica de hidrógeno. Reunión Anual AFA 2013. Bariloche, Argentina.

Haves-Labruto, L., Schillebeeckx, S.D.J., Workman, M., Shah, N., 2013. Contrasting perspectives on China's rare earth policies: reframing the debate through a stakeholder lens. Energy Policy 63, 55-68.

Huston, E.L., Sandrock, G.D., 1980. Engineering properties of metal hydrides. Journal of the Less Common Metals 74, 435-443.

Langford, J.L., Delhez, R., De Keijser, T.H.H., Mittemeijer, E.J., 1988. Profile analysis for microcrystalline properties by the Fourier and other methods. Australian Journal of Physics 41, 173-187.

Lottoskyy, M.V., Yartis, V.A., Pollet, B.G., Bowman Jr., R.C., 2014. Metal Hydride Hydrogen Compressors: A Review. International Journal of Hydrogen Energy 39, 5818-5851.

Lu, L., Lai, M.O., 1998. Mechanical alloying. Springer, New York. 137.

Massari, S., Ruberti, M., 2013. Rare earth elements as critical raw materials: Focus on international markets and future strategies. Resources Policy 38, 36-43.

Merkle, R., Maier, J., 2005. On the Tamman-Rule. Journal of Inorganic and General Chemistry 631, 1163-1165.

Obregón, S.A., Esquivel, M.R.., 2014. Scheme of thermal compression of hydrogen (TCH) using $MmNi_{4.25}Al_{0.75}$ recovered with ethyl alcohol and handled under non protective atmospheres. International Journal of Hydrogen Energy 39, 8577-8581.

Obregón, S.A., Andrade-Gamboa, J.J., Esquivel, M.R., 2012. Synthesis of Al-containing $MmNi_5$ by mechanical alloying: milling stages, structure parameters and thermal annealing. International Journal of Hydrogen Energy 37, 14972-14977.

Obregón, S.A., Andrade-Gamboa, J.J., Esquivel, M.R. 2012. On the Al-content and characterization of $MmNi_{5-x}Al_x$ synthesized by mechanical alloying. Procedia Materials Science 1, 156-163.

Palmer, P.E., Burkholder, H.R., Beaudry, B.J., Gschneidner Jr, K.A., 1992. The preparation and some properties of pure mischmetal. Journal of the Less Common Metals 87, 135-148.

Rodriguez-Carvajal, J., 1990. Satellite Meeting on Powder Diffraction. In Proceedings of the XV Congress of the International Union of Crystallography. Tolouse, France. 127.